JOURNAL OF AGRICULTURAL AND FOOD CHEMISTRY

Effect of Sucrose Ester Addition on Nucleation and Growth Behavior of Milk Fat−Sunflower Oil Blends

MARINA CERDEIRA,† SILVANA MARTINI,† RICHARD W. HARTEL,‡ AND MARIA LIDIA HERRERA*,†,§

Centro de Investigación y Desarrollo en Criotecnología de Alimentos, Calle 47 y 116, 1900 La Plata, Buenos Aires, Argentina, and Food Science Department, University of Wisconsin−Madison, 1605 Linden Drive, Madison, Wisconsin 53706

The effects of addition of the sucrose esters (SE) P-1670, P-170, and S-170 to a high-melting fraction of milk fat (HMF) and its blends with sunflower oil (SFO) on nucleation and growth were studied by laser polarized light turbidimetry and polarized light microscopy (PLM). The three SE delayed nucleation of HMF at the temperatures selected. P-1670 did not modify average crystal size after 3 h at crystallization temperature (T_c) or crystal size distribution and modified crystallization kinetics only slightly. P-170 and S-170, however, markedly diminished crystal size and narrowed crystal size distribution. Activation free energies of nucleation at equivalent supercooling, calculated using the Fisher−Turnbull equation, significantly increased with addition of SE. According to these results, among the mechanisms described in the literature for fats or emulsions, the cocrystallization hypothesis is the one that better described the effects of sucrose esters on crystallization behavior in these systems.

KEYWORDS: High-melting milk fat fraction; sunflower oil; sucrose esters; hydrophilic−lipophilic balance (HLB); nucleation; growth; cocrystallization mechanism

INTRODUCTION

Milk fat fractions find increasing application in a variety of food products. The high melting point stearins are useful in puffy pastry, whereas the midfractions are useful in Danish cookies. Stearins are also used in the reduction of the blooming properties of chocolate (*1*). Modification of high melting point stearins by blending with vegetable oils is becoming increasingly important because shortenings with good nutritional properties, which are free of trans fatty acids and rich in polyunsaturated fatty acids, can be obtained. Roy and Bhattacharyya (*2*) simulated a hydrogenated fat product by blending palm stearins with liquid oils, such as sunflower, soybean, and rapeseed. Pal et al. (*3*) modified butter stearin by blending it with sunflower and soybean oil to make fats with desired physical properties and fatty acid compositions suitable for utilization in a variety of food products.

Sucrose esters (SE) can be used in foods as emulsifiers because they are nontoxic, tasteless, and odorless and are digested to sucrose and fatty acids in the stomach. They can also be used in pharmaceuticals, cosmetics, and other products in which a nonionic, biodegradable emulsifier is required (*4*). Emulsifiers are useful functional additives without which many food products would be impossible to make. Emulsifiers typically act in multiphase systems in two main ways. The first is as an emulsifying agent to enable two distinct phases to be combined in a stable quasi-homogeneous state for an indefinite length of time. The second function of an emulsifier is often to modify the behavior of the continuous phase of a food product so as to bring about a specific effect or benefit. For example, the use of lecithin in chocolate reduces the viscosity of the product and improves the ease of handling and processability. SE have a common feature that makes them suitable as emulsifying agents: they are ambiphilic, possessing both lipophilic and hydrophilic properties. The nature of this property is often expressed as the hydrophilic/lipophilic balance (HLB) on a scale of 0 to 20, with low numbers indicative of the oil-like tendency (*5*). In addition to their major function of producing and stabilizing emulsions, SE contribute to numerous other functional roles as texturizers and film formers. Typical applications are baked goods, fruit coatings, and confectionery (*6*). Their role as fat crystallization modifiers has yet to be explored.

There are very few reports about the effect of SE on crystallization processes and development of polymorphic forms of fats in bulk systems (*7*−*9*). Recently, the effects of SE on lipid crystallization in emulsions were investigated (*10*−*12*). However, it is of great interest to study the effects of SE on bulk fat systems, particularly in regard to their use in products

* Address correspondence to this author at the Departamento de Industrias, University of Buenos Aires, Intendente Güiraldes S/N, 1428 Buenos Aires, Argentina (telephone 54-11-4576-3300, int. 274; fax 54-11-4576-3366; e-mail Lidia@di.fcen.uba.ar).
† Centro de Investigación y Desarrollo en Criotecnología de Alimentos.
‡ University of Wisconsin−Madison.
§ Associate Researcher of the National Research Council (CONICET).

10.1021/jf034011y CCC: $25.00
Published on Web 09/18/2003

Table 1. Chemical Composition and Mettler Dropping Points (MDP) of High-Melting Milk Fat Fraction (HMF), Sunflower Oil (SFO), and Their Blends

	chemical composition of starting materials[a] (wt %)				
acyl carbon	SFO	HMF	20% SFO	40% SFO	60% SFO
C26	0.1	0.2	0.2	0.1	0.2
C28	0	0.3	0.2	0.1	1.0
C30	0	0.7	0.4	0.4	0.2
C32	0	1.5	1.1	0.7	0.5
C34	0	2.9	2.4	1.7	1.1
C36	3.2	3.8	4.5	3.4	2.1
C38	1.8	6.0	7.5	6.0	4.1
C40	0	4.7	4.5	2.6	2.1
C42	0	4.6	4.0	3.0	1.9
C44	0	4.8	4.7	3.9	2.5
C46	0	6.9	7.9	5.7	3.9
C48	0	16.9	11.8	8.3	6.1
C50	1.3	23.4	14.6	12.1	9.0
C52	15.1	15.9	14.1	13.8	13.8
C54 (18:0)	1.1	1.5	0.9	1.0	0.00
C54 (18:1 cis)	76.0	1.4	16.8	32.1	50.2
C54 (18:1 other)	0	4.6	4.5	4.9	1.3
MDP (°C)		48.4	46.2	44.4	41.5

[a] Standard deviations for all values were <±1%.

such as chocolate and confections. The purpose of this work was to evaluate the effect of several SE with a range of HLB values on the nucleation and growth behavior of high-melting milk fat fraction−sunflower oil blends and to interpret changes in crystallization behavior in terms of the mechanisms described in the literature for emulsifiers' action.

MATERIALS AND METHODS

Starting Materials. High-melting milk fat fraction (HMF) was obtained from Grassland Dairy (Greenwood, WI) and sunflower oil (SFO) from Molinos Rio de La Plata S.A. (Avellaneda, Buenos Aires, Argentina). The HMF used in this study had a solid fat content of 82% at 5 °C and 67% at 20 °C, which corresponds to a very high melting fraction. The HMF was produced from anhydrous milk fat (AMF) using the Tirtiaux fractionation process. The fractionation process is a simple physical process that employs no additives. The AMF was heated until fully melted, cooled under controlled conditions to 45 °C, and pressure filtered to separate HMF from the remaining liquid fat. The fraction is not further processed after fractionation.

Three blends were prepared by mixing 20, 40, and 60% of SFO with HMF. Dropping points (the temperature at which a solid fat just begins to flow under controlled conditions) of the samples were determined with the Mettler FP 80 dropping point apparatus (Mettler Instruments A.G., Greifensee-Zurich, Switzerland), using a heating rate of 1 °C/min. Chemical composition and Mettler dropping points of all samples are reported in **Table 1**. Palmitic SE (P-170) with HLB = 1, stearic SE (S-170) with HLB = 1, and palmitic SE (P-1670) with HLB = 16 were supplied by Mitsubishi-Kasei Food Corp. (Tokyo, Japan). The SE had Mettler dropping points of 58.0, 59.5, and 44.0 °C, respectively. Monoester contents of S-170 and P-170 were 1 wt %, with di-, tri-, and polyesters comprising 99 wt %. P-1670 had 80% monoester and 20% di-, tri-, and polyester. SE were added at concentrations of 0.1 or 0.5 wt % to HMF and the three blends with SFO. Selected concentrations were within the concentrations usually employed in foods for these esters.

Laser Polarized Light Turbidimetry. The crystallization process was monitored by using an optical setup described elsewhere (*13*). A laser polarized turbidimeter with a helium−neon laser as light source was used to follow the occurrence of optically anisotropic fat crystals. The sample, ~80 g, was contained in a water-jacketed glass cell. A polarizer lens was placed between the laser and the cell. The temperature of the glass cell was controlled by means of water that was circulated from a water bath. The light transmitted by the crystals was then passed through the second analyzer placed at the Cross−Nicolls position with the first analyzer (at 90°); this enables the photodiode to detect crystals. A typical photosensor output and the cell temperature record were reported previously (*13*). Induction time of crystallization (τ) is defined as the interval between the moment crystallization temperature (T_c) is reached and the start of crystallization (first deviation from the laser baseline signal).

Thermal Treatments. Samples were melted and held at 80 °C for 30 min and then immediately placed in the glass cell at the set T_c reported in **Figure 1** with an agitation rate of 100 rpm. The cooling rate was calculated from the slope of the cell temperature record, and the results of several runs were averaged. A cooling rate of 5.5 ± 0.5 °C/min was obtained in all cases. Experiments were carried out in triplicate, and induction times were reported as the average. Differences in induction times between two samples were compared using the paired Student's t test at $P < 0.01$ and $P < 0.05$. In this study on mixtures of HMF and SFO, no effect of cooling rate on crystalline microstructure was observed, in contrast to our previous study on mixtures of HMF and SFO (*15*). Typically, the effects of processing conditions are minimized when crystallization driving force is high, as happens in the systems studied here formulated with a very high melting stearin. For this reason only one crystallization rate was reported. When the laser signal reached its peak (first crystals), the sample was filtered under vacuum with a Büchner filter using Whatman no. 4 filter paper (*15*). The solids on the filter cake were then analyzed for polymorphic form by X-ray diffractometry, for melting behavior by differential scanning calorimetry, and for chemical composition by capillary gas chromatography.

Calculation of Activation Free Energy of Nucleation. The activation free energy of nucleation, ΔG_c, was evaluated using the Fisher−Turnbull equation (*14*)

$$J = (NkT/h)\exp(-\Delta G_d/kT)\exp(-\Delta G_c/kT) \quad (1)$$

where J is the rate of nucleation, ΔG_d is the activation free energy of diffusion, k is the gas constant per molecule, T is the temperature, N is the number of molecules per cubic centimeter in the liquid phase, and h is Planck's constant. J can be taken as being proportional to the inverse of the induction time (τ) of nucleation. For a spherical nucleus, the activation free energy of nucleation is related to the surface free energy of the crystal/melt interface, σ, and the supercooling, defined as the melting point minus the crystallization temperature ($\Delta T = T_m - T_c$), by

$$\Delta G_c = (16/3)\pi\sigma^3 T_m^{\,2}/(\Delta H)^2(\Delta T)^2 \quad (2)$$

with ΔH the enthalpy of nucleation.

As fats do not undergo glass transition, there are no dramatic changes in viscosity in the temperature range within which there is induction time for nucleation. In addition, crystallization in fats systems is not a diffusion-controlled process. Therefore, for a triacylglycerol system, the main barrier for incorporation in a nucleus is the molecular conformation and, therefore, the first exponential in eq 1 (energy of diffusion) is equal to

$$-\alpha\Delta S/R \quad (3)$$

where α is the fraction of molecules that should be in the right conformation for incorporation in a nucleus, ΔS is the decrease of entropy on crystallization of 1 mol of TAG, and R is the gas constant. Combining eqs 1−3 and rearranging, the following equation is obtained:

$$\tau T = h/\mathrm{N}k\exp(\alpha\Delta S/k)\exp[(16/3)\pi\sigma^3 T_m^{\,2}/kT(\Delta H)^2(\Delta T)^2] \quad (4)$$

From a plot of $\ln \tau T$ versus $1/T(\Delta T)^2$, a slope (s) can be evaluated, which allows calculation of the activation free energy of nucleation from

$$\Delta G_c = sk/(T_m - T_c)^2 \quad (5)$$

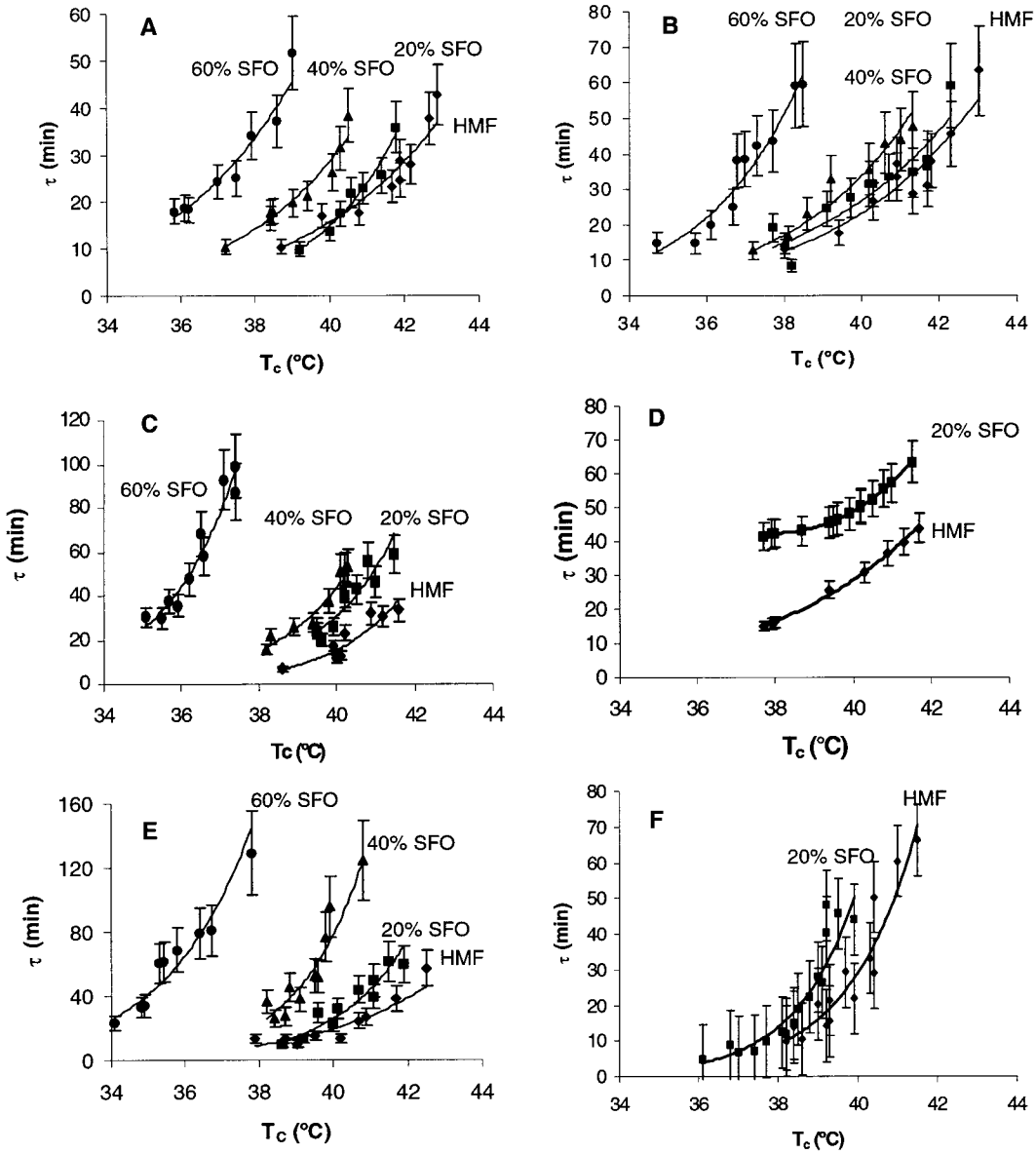

Figure 1. Induction times of crystallization versus temperature for all samples: (A) without sucrose esters; (B) with P-1670 0.1 wt %; (C) with P-170 0.1 wt %; (D) with P-170 0.5 wt %; (E) with S-170 0.1 wt %; (F) with S-170 0.5 wt %. Data points are the average of three runs. Error bars are standard deviations.

Although the slope obtained from this analysis is a constant, the activation free energy is a function of supercooling. The Fisher−Turnbull equation was originally derived for a single-component system; however, it was proved to be applicable to multicomponent systems such as palm and sunflower oils (*16*, *17*).

Light Microscopy. Crystals were observed with a polarized light microscope (Nikon Optiphot, Garden City, NY) equipped with a video camera connected to a computer. Optimas 6.1 (Optimas, Bothell, WA) software was used to collect the images. At the point when the sample temperature reached the crystallization temperature, samples were taken for PLM observation, with sampling continuing until crystallization was completed (3 h). At each sample point, a drop of slurry was placed between a warmed slide and a cover slide. Images were taken in duplicate at every sample time with a 10× objective and a TV relay ocular lens. After 3 h, at least 20 images had been taken. The individual areas of crystals were measured using the Optimas software, and the results were exported to Microsoft Excel 7.0 (Microsoft, Redmond, WA) software for graphic presentation of data. From 200 to 300 crystals were measured for each sample. The diameters of circles having areas equivalent to the measured areas were reported.

X-ray Diffraction (XRD). The polymorphic forms of the initial crystals formed were analyzed by using a Philips 1730 X-ray spectrometer fitted with a system for temperature control (Philips Argentina S.A., Capital Federal, Argentina). The temperature of the sample holder placed within the refraction chamber was controlled through a programmable Lauda UK 30 cryostat (Werklauda, Königshofen, Germay). Ethylene glycol in water (3:1, v/v) was used as coolant. Kα1α2 radiation from copper was used at 40 kV, 20 mA, and a scanning velocity of 1°/min from 5 to 30°.

Differential Scanning Calorimetry (DSC). Melting profiles were measured in a Polymer Laboratories calorimeter (Rheometric Scientific Ltd.) driven with Plus v 5.41 software. Calibration was carried out at a heating rate of 10 °C/min by using indium proanalysis (p.a.), lauric acid p.a., and stearic acid p.a. as standards. From 5 to 9 mg of each sample in hermetically sealed aluminum pans was placed in the DSC and held at −10 °C for 5 min prior to melting at a heating rate of 10 °C/min from −10 to 80 °C. A single empty pan was employed as a reference. Three replicates were performed for each sample, and means and standard deviations of peak temperatures and melting enthalpies are reported.

GC Analysis. The acyl carbon profile of samples was determined with a Hewlett-Packard 5890 series II (Hewlett-Packard, San Fernando, CA) gas chromatography (GC) unit equipped with a flame ionization detector (FID) and on-column injector. The column used was a Heliflex

Phase AT-1 with a length of 30 m and an internal diameter of 0.25 mm (Alltech Associates, Deerfield, IL). Helium was the carrier gas at a flow rate of 2 mL/min with hydrogen gas and air also being supplied to the FID. Samples were prepared by using a modified method of Lund (*18*). A sample of 10 mg was weighed in GC vials and dissolved in 1.8 mL of iso-octane with 100 μL of internal standard (C27 in iso-octane: 2.02 mg/mL). Samples were stored in a refrigerator prior to analysis. To separate the different TAG according to acyl carbon number, the following temperature profile was used in the GC: initial hold at 280 °C for 1 min followed by heating at a rate of 3.0 °C/min until a temperature of 355 °C was reached. The detector was held constant at 370 °C. Composition (area percent) was based on the area integrated by using ChemStation chromatography software by Hewlett-Packard. Samples were run in duplicate.

RESULTS AND DISCUSSION

Effect of Sucrose Esters on Induction Times of Crystallization. Figure 1 shows the induction times for HMF and blends crystallized without emulsifiers and with the addition of the sucrose esters P-170 and S-170 at 0.1 and 0.5 wt % levels and P-1670 at 0.1 wt % level. Induction times obtained for P-1670 at 0.1 wt % are reported here, because this sucrose ester was not soluble in the fat systems used in this study at 0.5 wt %. For all samples with and without emulsifiers, a continuous curve can be drawn for induction time versus temperature figures. As was previuosly reported (*15*) this means that when samples were crystallized at these temperatures, only one polymorphic form was expected.

For samples without SE, it was necessary to add at least 40% SFO to HMF to obtain induction times significantly different between HMF and a selected blend at $p < 0.05$ (**Figure 1A**). The addition of P-1670 at 0.1 wt % level to HMF and the blends delayed crystallization at $p < 0.05$ (**Figure 1B**). There were significant differences ($p < 0.05$) in induction times for HMF with the addition of P-170 or S-170 at 0.1 or 0.5 wt % level (**Figure 1C**,**D**, respectively). Significant differences ($p < 0.05$) for the 20% SFO blend with the addition of P-170 or S-170 at 0.1 or 0.5 wt % level were also found (**Figure 1E**,**F**). In all cases, P-170 and S-170 delayed nucleation at both concentrations. Nucleation was very significantly delayed ($p < 0.01$) for 40 and 60% SFO blends with P-170 and especially with S-170 at 0.1 wt %. At the 0.5 wt % level, both P-170 and S-170 delayed nucleation of the 40 and 60% SFO blends to a greater extent, with no crystallization observed even after 7 h at all temperatures selected for this study.

Two mechanisms have been reported in the literature to interpret the effects of emulsifiers on fat crystallization in bulk systems. First, the emulsifiers can act as heteronuclei, accelerating nucleation through the catalytic actions of such impurities. During crystal growth, the emulsifiers are adsorbed at steps or kinks on the surface of growing fat crystals and, thereby, inhibit crystal growth and modify crystal morphology. Second, fats and emulsifiers are able to cocrystallize because of their somewhat similar chemical structures. However, the structural dissimilarities between triacylglycerols and emulsifiers can delay nucleation and inhibit growth. In general, an emulsifier with a high molecular weight and the above-mentioned chemical characteristics has the potential to be a good inhibitor of crystallization (*19*). In emulsion systems, another accelerating mechanism has also been observed. S-170 and P-170 are absorbed at the oil−water (O/W) interface and may accelerate the heterogeneous nucleation of the oil phase at the surface of the droplets when the O/W emulsion is cooled (*11*). However, this type of acceleration with added hydrophobic emulsifiers on nucleation has not been observed in bulk fat systems (*20*).

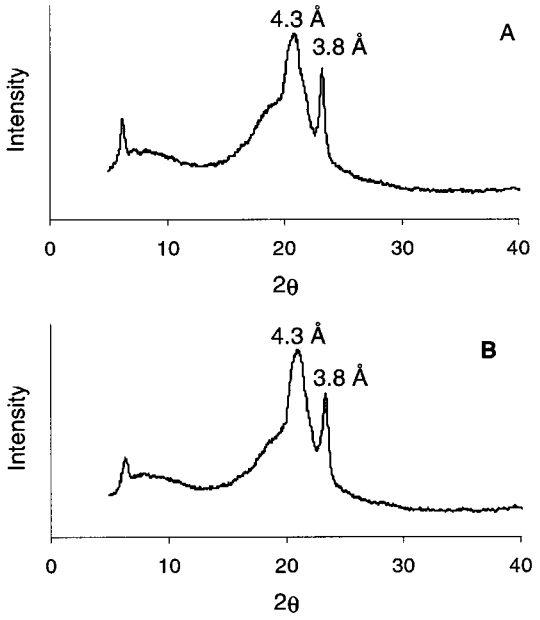

Figure 2. X-ray patterns of initial crystals of (A) 20% SFO and (B) 20% SFO with addition of P-170 at 0.5 wt % crystallized at 38.5 °C.

The SE selected for this study were formed by interesterification of sucrose and the fatty acids palmitic (P) and stearic (S), which are present in high proportions in milk fat. P-1670 has low affinity for hydrophobic compounds (HLB = 16). It might have been expected that P-1670 would not cocrystallize with the fat phase and might act as an impurity to accelerate crystallization (*20*). Despite its hydrophilicity, P-1670 is soluble in the fat system at the concentration used in this study. Its melting point (44 °C) is lower than those of P-170 and S-170 but still high enough to cocrystallize with the fat. In addition, the presence of palmitic acid in P-1670, which is a main fatty acid in milk fat, made it efficient at delaying nucleation at the temperatures selected for this study. P-170 has a high affinity for hydrophobic compounds (HLB = 1) and chemical groups similar to the fat system in which it was crystallized. P-170 also has a high melting point (MDP = 58 °C). Therefore, P-170 may be expected to cocrystallize with HMF−SFO blends and delay crystallization. S-170 has the same HLB value as P-170, but stearic acid is present at a lower percentage than palmitic acid in milk fat. However, as SFO was added, the percentage of C_{54} carbon number increased (**Table 1**), and because molecular interactions are easier between compounds with the same chain length, S-170 becomes very efficient in delaying nucleation. Thus, S-170 delayed crystallization to a greater extent than P-170 at 0.1 wt % for 40 and 60% SFO blends. From these results, among the mechanisms described in the literature, the cocrystallization hypothesis is the one that seems to better describe the effects of SE on crystallization behavior in the systems used in this study.

Polymorphic Behavior. For all samples, both with and without addition of P-1670 at the 0.1 wt % level and P-170 and S-170 at the 0.1 and 0.5 wt % levels, a continuous curve can be drawn for induction time versus temperature. Therefore, only one polymorphic form is expected. These results were confirmed by analyzing the initial crystals by X-ray diffraction. For all samples at all T_c, both with and without SE, only the β'-form was found. As shown in **Figure 2**, the patterns were characteristic of the β'-form with two strong signals at 3.9 and 4.3 Å. No signal at 4.6 Å, characteristic of the β-form, was found. X-ray spectra for all samples with and without SE were

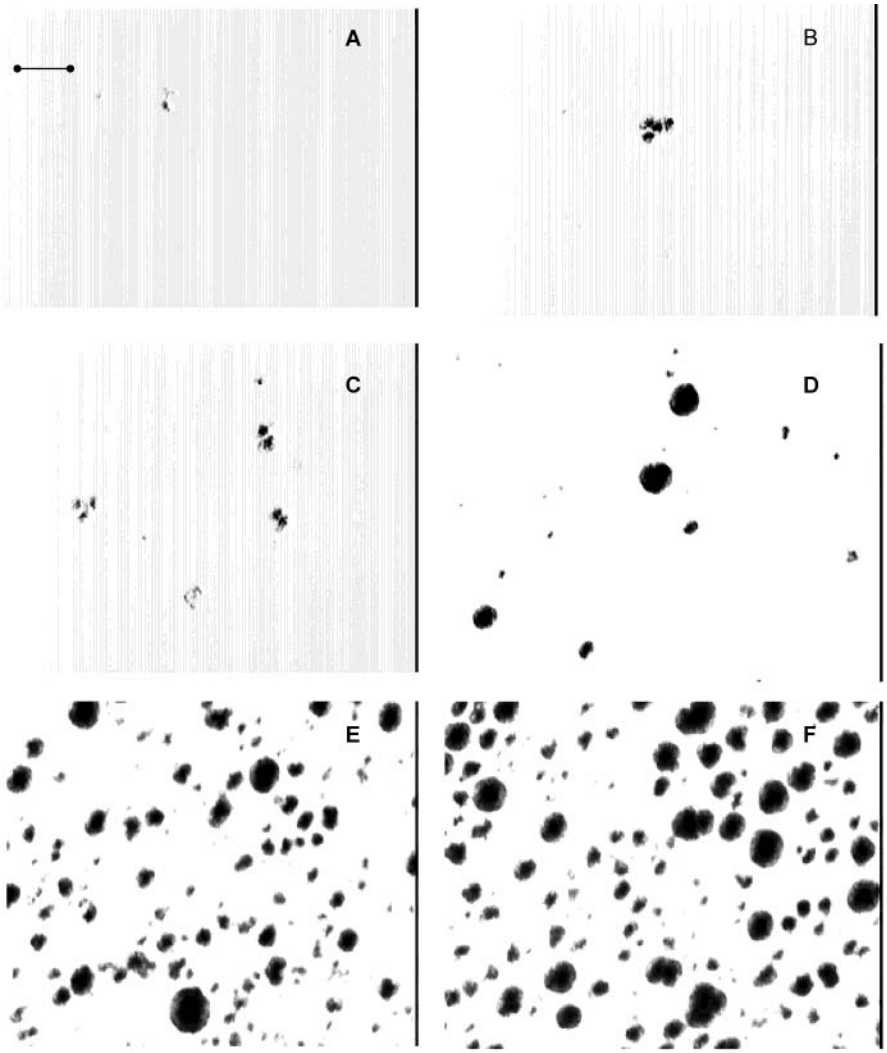

Figure 3. Images of crystals corresponding to the 20% SFO blend crystallized at 38 °C. Images were taken at (A) 2, (B) 4, (C) 7, (D) 11, (E) 19, and (F) 22 min.

very similar and, therefore, polymorphism was not responsible for the differences in induction times found when SE were added to HMF and the blends. Studies of the crystallization of palm midfraction (PMF) in an emulsion system reported that with the addition of S-170, PMF preferentially crystallized in the β'-form. The α-form was found to crystallize below its melting point, 13 °C, when a sucrose ester was added (*10*). This effect on polymorphism was not found in the bulk systems formulated with HMF and SFO.

Polarized Light Microscopy Studies. To confirm the hypothesis of cocrystallization, samples were taken from the crystallizer beginning when the samples reached crystallization temperature and continuing until crystallization was complete. As an example, **Figure 3** shows how the crystals changed with time for the 20% SFO blend crystallized at 38 °C, and **Figure 4** shows changes for the 20% SFO blend with the addition of P-170 at the 0.1 wt % level at the same temperature. Despite the low concentration of P-170 (0.1%), crystallization of the 20% SFO blend was inhibited as evidenced by the longer induction times observed with PLM, confirming laser polarized turbidimetry results. This effect was even more obvious for 40 and 60% SFO blends. P-170 had a dramatic effect on crystal size, favoring the formation of more and smaller initial crystals (**Figures 3** and **4**). However, it had no effect on crystal morphology. In general, this behavior was observed for all samples with the addition of P-170 and S-170 at 0.1 wt %. It was even more significant for HMF and 20% SFO at the 0.5 wt % addition level ($p < 0.01$). S-170 had a greater effect on crystal size than P-170. Crystal size was markedly smaller in agreement with the most efficient effect in delaying nucleation. The 40 and 60% blends did not crystallize after 7 h with both SE at the 0.5 wt % level. For all samples and at all T_c, no significant differences in crystal size were found for P-1670 ($p < 0.05$).

Crystal Size Distribution. As an example, **Figure 5** shows crystal size distributions for the 20% SFO blend (A) without SE and (B) with P-170 at 0.1 wt % after 3 h of crystallization at 38 °C. Mean and standard deviation of the distributions were 12.5 ± 4.1 and 10.1 ± 2.7 μm for 20% SFO and 20% SFO with 0.1 wt % of P-170, respectively. At a concentration of 0.5 wt %, the mean size was 7.2 ± 2.0 μm (data not shown). The longer induction times for crystallization upon addition of P-170 led to smaller crystal size. In nucleation, molecules need sufficient time to organize and align with their neighbors to form stable nuclei. When induction times are elongated, as is the case of addition of P-170 to the 20% SFO blend, that organization takes place for more time at crystallization temperature. As a result, smaller sized crystals with a narrow distribution are obtained, with nucleation rates larger relative to the growth rate of the crystals. This effect was previously observed for any factor that delays nucleation (*21*). The same results were obtained for all samples for addition of P-170 and

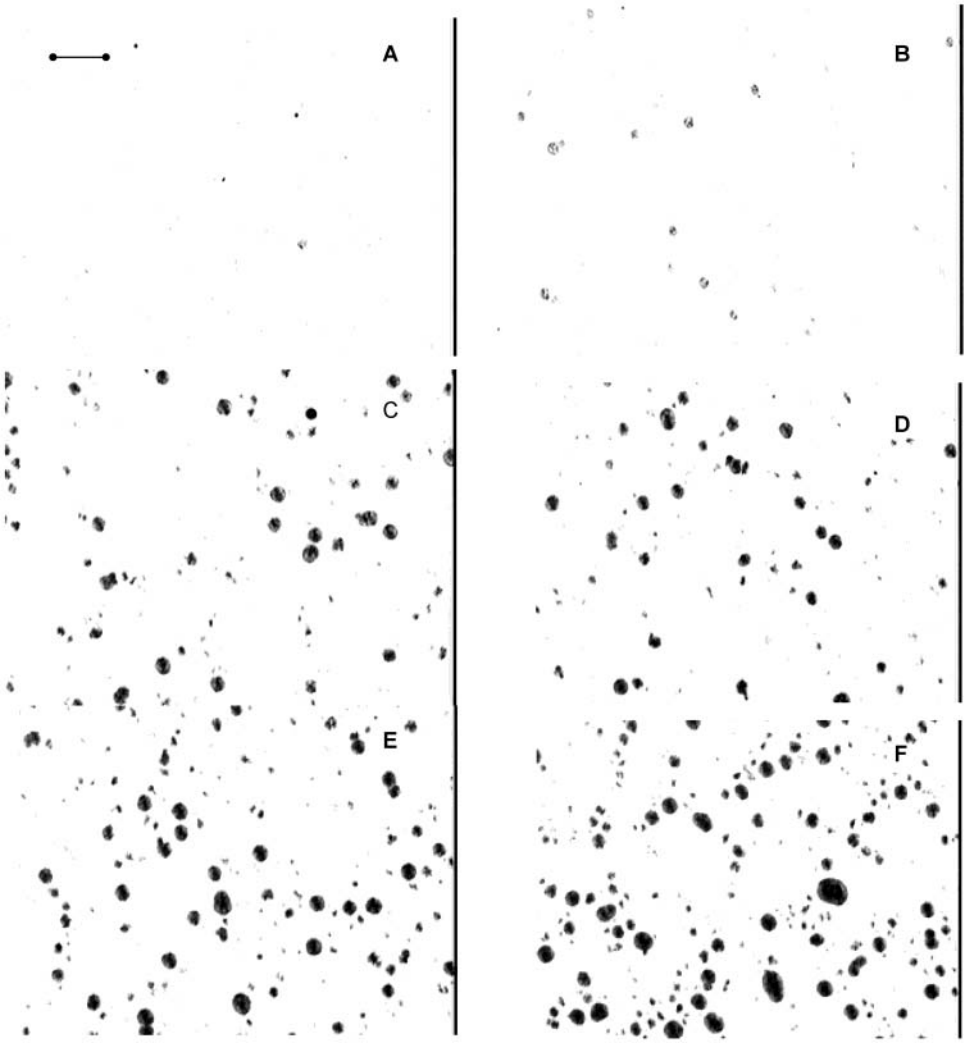

Figure 4. Images of crystals corresponding to the 20% SFO blend with P-170 at 0.1 wt % crystallized at 38 °C. Images were taken at (A) 15, (B) 17, (C) 20, (D) 25, (E) 32, and (F) 40 min.

S-170 at the 0.1 wt % level and for HMF and 20% SFO at the 0.5 wt % level. However, there were no significant differences between HMF or the blends and the samples with P-1670. The results obtained in PLM studies support a cocrystallization mechanism, because at the concentrations selected, the main effect was a delay on nucleation. Crystal morphology was not modified by the addition of SE, indicating that the growth mechanism was not modified.

Melting Behavior of Initial Crystals. Figure 6 shows the melting thermograms coresponding to 20 and 40% SFO and with P-170 at 0.1 or 0.5 wt % to document the effect of SE on melting behavior, and **Table 2** shows peak enthalpies and onset temperatures for all curves. As reported in **Table 2**, samples with P-170 at 0.1 or 0.5 wt % had slightly higher melting enthalpies than samples without SE in all cases ($p < 0.05$). The same results were obtained for S-170. Higher levels of P-170 generally led to initial crystals with less (1.0−2.5%) TAG with acyl carbon numbers between C_{34} and C_{40} and more (1.0−3.7%) TAG with acyl carbon numbers from 46 to 54. This behavior was general for all samples. Even though there were slight differences in chemical composition between samples with and without emulsifiers, addition of P-170 or S-170 at 0.5 wt % increased onset temperature significantly for HMF or the 20% SFO blend ($p < 0.05$) and addition of P-170 or S-170 at 0.1 wt % significantly increased onset temperatures for 40 or 60% SFO blends ($p < 0.05$). The slightly higher content of larger TAG (higher acyl carbon number) may not be the only explanation for onset temperature changes. Interactions between TAG and SE should also play a key role in the increase of melting enthalpies and onset temperatures.

Activation Free Energies of Nucleation. As an example, the activation free energies (ΔG_c) of all samples without emulsifiers and with S-170 at 0.1 and 0.5 wt %, calculated from the Fisher−Turnbull equation and with the induction times reported in **Figure 1**, are shown in **Table 3** along with the crystallization temperatures and supercoolings, $\Delta T = (T_m - T_c)$. The MDP was used as T_m. The slopes obtained from plots of $\ln(\tau T)$ versus $1/T(\Delta T)^2$ for the HMF and 10, 20, and 40% SFO samples were 7732, 5096, 3040, and 1194, respectively, 11976, 6217, 6130, and 5332 for these samples with S-170 0.1 wt %, and 38907 and 17232 for HMF and the 20% SFO blend with S-170 0.5 wt %, respectively. The regression coefficients obtained from the plots varied from 0.91 to 0.95. The ΔG_c of HMF and the 20% SFO blend significantly increased ($p < 0.05$) as the amount of P-170 or S-170 increased for the same supercooling (i.e., for a ΔT of 9.6 °C ΔG_c values were 0.3, 0.5 and 3.4 kJ/mol for HMF, HMF with S-170 0.1%, and HMF with S-170 0.5%, respectively). The 40 and 60% blends did not crystallize with P-170 or S-170 at the 0.5% level. For these samples P-170 or S-170 at 0.1% significantly increased ΔG_c values ($p < 0.05$). Although P-1670 did not modify crystal size and crystal size distribution, it significantly increased ΔG_c for

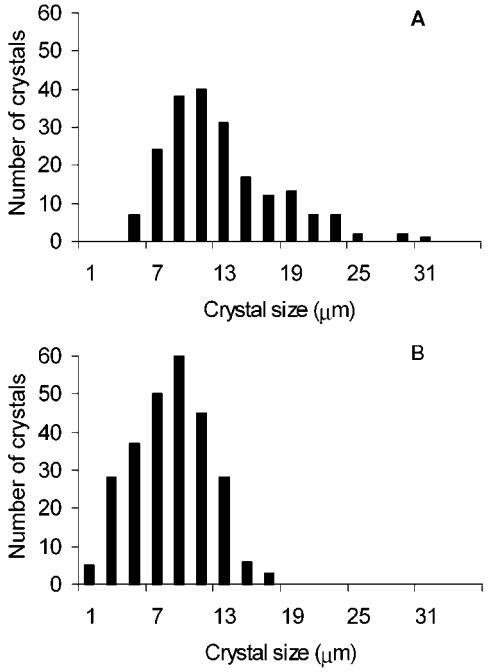

Figure 5. Crystal size distribution of (A) 20% SFO and (B) 20% SFO with P-170 0.1 wt % crystallized at 38 °C for 3 h.

Table 2. Onset Temperatures and Peak Enthalpies of the 20 and 60% SFO Blends with and without P-170

sample	onset temp (°C)	peak enthalpy (mJ/mg)
20% SFO	62.4 ± 3.5	44.1 ± 2.1
20% SFO P-170 0.1 wt %	65.2 ± 2.0	45.9 ± 1.0
20% SFO P-170 0.5 wt %	71.6 ± 0.4	47.0 ± 0.2
60% SFO	72.0 ± 0.5	48.9 ± 0.4
60% SFO P-170 0.1 wt %	74.4 ± 1.2	50.1 ± 0.6

all samples ($p < 0.05$), which is not surprising taking into account that it elongated induction times for crystallization.

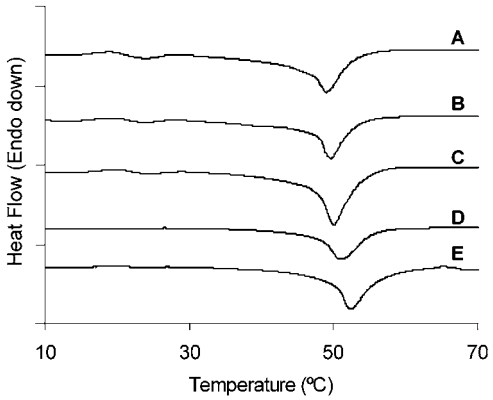

Figure 6. DSC melting diagrams of initial crystals obtained by dry filtering at 38.5 °C: (A) 20% SFO; (B) 20% SFO with addition of P-170 0.1 wt %; (C) 20% SFO with addition of P-170 0.5 wt %; (D) 60% SFO; (E) 60% SFO with addition of P-170 0.1 wt %.

Because of their somewhat similar chemical structures, the SE selected in this study were able to cocrystallize with the fats. However, the structural dissimilarities between triacylglycerols and emulsifiers were responsible for a delay in nucleation and an inhibition of growth. Activation free energies of nucleation were higher with the addition of SE in agreement with the fact that SE impeded nucleation.

ABBREVIATIONS USED

SE, sucrose esters; HLB, hydrophilic−lipophilic balance; P-170, palmitic acid sucrose ester HLB = 1; S-170, stearic acid sucrose ester HLB = 1; P-1670, palmitic acid sucrose ester HLB = 16; AMF, anhydrous milk fat; HMF, high-melting fraction of milk fat; SFO, sunflower oil; T_c, crystallization temperature; T_m, melting point; MDP, Mettler dropping point; TAG, triacylglycerol; PLM, polarized light microscopy; XRD, X-ray diffraction.

Table 3. Activation Free Energies of Nucleation of All Samples and with S-170 at 0.1 and 0.5 wt %[a]

HMF			20% SFO			40% SFO			60% SFO		
T_c (°C)	ΔT (°C)	ΔG_c (kJ/mol)	T_c (°C)	ΔT (°C)	ΔG_c (kJ/mol)	T_c (°C)	ΔT (°C)	ΔG_c (kJ/mol)	T_c (°C)	ΔT (°C)	ΔG_c (kJ/mol)
38.7	9.6	0.3	39.2	6.9	0.4	37.2	7.1	0.2	35.8	5.7	0.1
39.8	8.5	0.4	40	6.1	0.5	38.4	5.9	0.3	36.1	5.4	0.1
40.8	7.5	0.5	40.3	5.8	0.5	38.5	5.8	0.3	36.2	5.3	0.2
41.7	6.6	0.6	40.6	5.5	0.6	39.0	5.3	0.4	37.0	4.5	0.2
41.9	6.4	0.7	40.9	5.2	0.7	39.4	4.9	0.4	37.5	4.0	0.3
42.2	6.1	0.7	41.4	4.7	0.8	40.1	4.2	0.6	37.9	3.6	0.3
42.7	5.6	0.9	41.8	4.3	1.0	40.3	4.0	0.7	38.6	2.9	0.5
With Addition of S-170 0.1%											
37.9	10.4	0.4	38.6	7.5	0.4	38.2	6.1	0.6	34.1	7.4	0.3
38.7	9.6	0.5	39.2	6.9	0.5	38.4	5.9	0.6	34.5	7.0	0.4
39.5	8.8	0.6	39.6	6.5	0.5	38.7	5.6	0.7	34.8	6.7	0.4
40.7	7.6	0.7	40.7	5.4	0.7	38.8	5.5	0.7	34.9	6.6	0.5
40.9	7.4	0.8	41.1	5.0	0.9	39.1	5.2	0.8	35.3	6.2	0.5
41.7	6.6	1.0	41.5	4.6	1.0	39.5	4.8	0.9	35.4	6.1	0.5
42.5	5.8	1.3	41.9	4.2	1.2	39.6	4.7	1.0	35.8	5.7	0.6
With Addition of S-170 0.5%											
36.4	12.0	2.3	37.9	8.3	2.1	36.8	7.6	NC[b]	32.5	9.0	NC
37.7	10.7	2.8	38.1	8.1	2.2	37.4	7.0	NC	32.7	8.8	NC
38.0	10.4	3.0	38.5	7.7	2.4	38.0	6.4	NC	33.1	8.4	NC
38.2	10.2	3.1	38.8	7.4	2.6	38.6	5.8	NC	33.7	7.8	NC
39.1	9.3	3.8	39.2	7.0	3.0	39.1	5.3	NC	34.3	7.2	NC
39.5	8.9	4.1	39.5	6.7	3.2	39.5	4.9	NC	34.9	6.6	NC
40.1	8.3	4.7	39.9	6.3	3.7	39.9	4.5	NC	35.1	6.4	NC

[a] Values that differ more than 10% are significantly different at $p<0.05$. [b] No crystallization occurred after 7 h at crystallization temperature (T_c).

ACKNOWLEDGMENT

We acknowledge the University of Wisconsin—Madison for its Exchange Visitor Program P 1 0105. S.M. is grateful to the National Research Council of Argentina (CONICET) for a Ph.D. scholarship.

LITERATURE CITED

(1) Kellens, M. Developments in fractionation techniques. In *Treatise in Fats, Fatty Acids and Oleochemicals*; Narula, O. P., Ed.; Industrial Consultants: New Delhi, India, 1997; Section B1, Chapter 7, p 15.

(2) Roy, S.; Bhattacharyya, D. K. Comparative nutritional quality of palm stearin liquid oil blends and hydrogenated fat (vanaspati). *J. Am. Oil Chem. Soc.* **1996**, *73*, 617−622.

(3) Pal, P. K.; Bhattacharyya, D. K.; Ghosh, S. Modifications of butter stearin by blending and interesterification for better utilization in edible fat products. *J. Am. Oil Chem. Soc.* **2001**, *78*, 31−36.

(4) Gupta, R. K.; James, K.; Smith, F. J. Sucrose esters and sucrose ester/glyceride blends as emulsifiers. *J. Am. Oil Chem. Soc.* **1983**, *60*, 862−869.

(5) Weyland, M. Emulsifiers in confectionery. In *Food Emulsifiers and Their Applications*; Hasenhuettl, G. L., Hartel, R. W., Eds.; Chapman and Hall: New York, 1997; pp 235−254.

(6) Hasenhuettl, G. L. Overview of food emulsifiers. In *Food Emulsifiers and Their Applications*; Hasenhuettl, G. L., Hartel, R. W., Eds.; Chapman and Hall: New York, 1997; pp 1−9.

(7) Yuki, A.; Matsuda, K.; Nishimura, A. Effect of sucrose polyesters on crystallization behavior of vegetable shortening and margarine fat. *J. Jpn. Oil Chem. Soc.* **1990**, *39*, 236−244.

(8) Herrera, M. L.; Marquez Rocha, F. J. Effects of sucrose ester on the kinetics of polymorphic transition in hydrogenated sunflower oil. *J. Am. Oil Chem. Soc.* **1996**, *73*, 321−326.

(9) Nasir, M. I. Effect of sucrose polyesters and sucrose polyester−lecithins on crystallization rate of vegetable ghee. In *Crystallization and Solidification Properties of Lipids*; Widlak, N., Hartel, R. W., Narine, S., Eds.; AOCS Press: Champaign, IL, 2001; pp 87−95.

(10) Awad, T.; Sato, K. Effects of hydrophobic emulsifier additives on crystallization behavior of palm mid fraction in oil-in-water emulsion. *J. Am. Oil Chem. Soc.* **2001**, *78*, 837−842.

(11) Katsuragi, T.; Kaneko, N.; Sato, K. Effects of addition of hydrophobic sucrose fatty acid oligoesters on crystallization rates of *n*-hexadecane in oil-in-water emulsions. *Colloids Surf. B: Biointerfaces* **2001**, *20*, 229−237.

(12) Awad, T.; Sato, K. Acceleration of crystallization of palm kernel oil in oil-in-water emulsion by hydrophobic emulsifier additives. *Colloids Surf. B: Biointerfaces* **2002**, *25*, 45−53.

(13) Herrera, M. L. Crystallization behavior of hydrogenated sunflowerseed oil: kinetics and polymorphism. *J. Am. Oil Chem. Soc.* **1994**, *71*, 1255−1260.

(14) Strickland-Constable, R. F. Nucleation of solids. In *Kinetics and Mechanism of Crystallization*; Academic Press: London, U.K., 1968; pp 74−129.

(15) Martini, S.; Herrera, M. L.; Hartel, R. W. Effect of cooling rate on nucleation behavior of milk fat−sunflower oil blends. *J. Agric. Food Chem.* **2001**, *49*, 3223−3229.

(16) Ng, W. L. A study of the kinetics of nucleation in a palm oil melt. *J. Am. Oil Chem. Soc.* **1990**, *67*, 879−882.

(17) Herrera, M. L.; Falabella, C.; Melgarejo, M.; Añón, M. C. Isothermal crystallization of hydrogenated sunflower oil: I—Nucleation. *J. Am. Oil Chem. Soc.* **1998**, *75*, 1273−1280.

(18) Lund, P. Butterfat triglycerides. *Milchwissenschaft* **1988**, *43*, 159−161.

(19) Garti, N. Effects of surfactants on crystallization and polymorphic transformation of fats and fatty acids. In *Crystallization and Polymorphism of Fats and Fatty Acids*; Garti, N., Sato, K., Eds.; Dekker: New York, 1988; pp 267−303.

(20) Garti, N.; Yano, J. The roles of emulsifiers in fat crystallization. In *Crystallization Processes in Fats and Lipid Systems*; Garti, N., Sato, K., Eds.; Dekker: New York, 2001; pp 211−250.

(21) Herrera, M. L.; Hartel, R. W. Effect of processing conditions on crystallization kinetics of a milk fat model system. *J. Am. Oil Chem. Soc.* **2000**, *77*, 1177−1187.

Received for review January 7, 2003. Revised manuscript received June 23, 2003. Accepted July 1, 2003. This work was supported by the National University of La Plata through Project 11/X279 and by the International Foundation for Science (IFS) of Sweden through Project E−3066-1.

JF034011Y